Dual-Frequency Interferometric SA R Observations of Tropical Rain-Forests.

Eric Rignot

Jet l'repulsion Laboratory, California Institute of Technology, Pasadena, *CA* 91109-8099

Phone: (818) 354-1640; Fax:(818) 354-0495; E-mail: eric@adelie.jpl.nasa.gov

Abstract

Repeat-pass, interferometric, radar observations of tropical rain-forests collected by the Shuttle Imaging Radar SIR-C in Rondonia, Brazil reveal C-band (5.6 -cm) radar signals completely decorrelate over the forest, whereas L-band (24-cm) signals remain strongly coherent over the entire landscape. At L-band, the difference in elevation between forest, and clearings is within the 8-m height noise of the data. Atmospheric delays are large, however, forming kilometer-sized anomalies with a 1.2-cm rms one way. Radar interferometric studies of humid tropics must be conducted at long radar wavelengths, with kilometric baselines or with two antennas operating simultaneously,

Introduction.

The recent advent of synthetic-aperture radar (S AR) interferometry to map the surface topography of land surfaces and to detect wavelength-sized changes in surface topography caused by natural events has stirred enormous interest for this technique in the scientific community. Surface topography of our planet is poorly known, especially in the tropics where digital topographic maps are almost nol(-existent, and SAR interferometry may offer the only promise to provide self-consistent, global, topographic maps (Zebker et al., 1994).

Knowing surface topography is extremely important for studying forested ecosystems. Elevation, slope and aspect exert enormous control on intercepted solar radiation, precipitation and runoff, river flooding, evaporation, soil moisture and vegetation type and health, Slope and aspect in digital form are also important for calibrating remote sensing satellite imagery used to study and monitor these regions.

Most results obtained to date with SAR interferometry nave utilized SAR data collected by the European ERS-1 satellite which operates a C-band frequency (5.6 cm wavelength) radar with vertical transmit and receive polarization. Although the success rate of ERS-1 repeat-pass interferometry has been fairly high over desert and polar ice sheets, several studies suggested temporal coherence of the SAR signal worsens considerably in the presence of vegetation, especially forests (e.g. Hagberg et al<, 1995).

The Shuttle Imaging Radar C (SIR-C) experiment provided the first opportunity to compare the merits and values of C- and 1,-band frequencies for repeat-pass radar interferometry applications over land. SIR-C collected interferometric data at a one-day repeat-pass cycle during the last few days of its second mission, covering large areas of the tropics. The images analyzed here were acquired at 10.61° south, 63.51° west, south of the city of Porto Velho and west of the city of Ariquemes, in the state of Rondonia, Brazil, on October 7, 8 and 9, 1994, during data take (1)"1') 119.4, 135.4 and 151.4 of the space shuttle. The radar image shown in Figure 1 (DT 119.4) is 46.1 km x 34.3 km in size, with the radar flying from left to right, looking to its left, 208 km above ground. The incidence angle of the radar illumination is 47.2° at the center. Spatial resolution is 44 m in range and 49 m in azimuth (along-track) after spatial averaging using 6 samples in range and 6 in azimuth. The images were acquired at 1,- (24 cm) and C-band (5,6 cm) frequencies, with vertical transmit and receive linear polarization.

The state of Rondonia has been characterized by spectacular deforestation in the 1970's and 1980's, thoroughly documented by optical sensors (Tucker et al., 1984). Large areas of tropical forests arc cleared every year to yield new pasture for raising cattle, along with a few subsidence cultivations. Cleared areas generally appear dark in radar images due to their low backscatter intensity, and are located along or close 10 roads.

Methods

As all modern SARS, the SIR-C instrument recorded the amplitude and phase of the radar returns expressed as a complex number for each image pixel. To form an interferogram, two successive images were registered and we computed the normalized cross-correlation coefficient of the complex amplitudes measured by the radar over the same surface elements. The magnitude of the resulting numbers measures the temporal coherence of the signal between O (no coherence) and 1 (perfect coherence). '1'heir phase measures the relative displacement of the surface elements along the radar line of sight between the two instances of imaging.

The phase coherence image of the pair combining DT (data take) 119,4 and 135.4 is shown in Figure 2 at L- and C-band. A similar image was obtained for DT 135.4 and 151.4. L-band coherence is high for the forest, (> 0,7) and for cleared areas (> 0.85). C-band coherence is only high for cleared areas (0.6) and very low (< 0,2) for the forest.

A height map obtained from the first pair of images is shown in Figure 3. The baseline was estimated using least square fitting and 50 tic-points from a published topographic map at 1:100,000. Between the first two passes, the baseline separation was B = 230 m, with an orientation angle α = -27° above horizontal, corresponding to a baseline component perpendicular to the radar illumination $B_\perp$ = 63 m, slowly varying along-track. For the

second pair, B was 114 **m** and α was 82.4°, **yielding** $B_\perp = 93$ m.

Sources of Signal Decorrelation

Factors influencing signal coherence may be separated into two categories: 1) system effects, and 2) surface effects. System effects include: 1) thermal noise, and 2) geometric decor-relation, These error sources are independent, and their effect on temporal coherence is multiplicative (Zebker and Villasenor, 1992).

For thermal noise, the multiplicative coherence coefficient is

$$\rho_{SNR} = 1/(1 + SNR^{-1}), \tag{1}$$

where SNR is the signal-to-noise ratio. To estimate the noise floor of the data, we utilized the backscatter level of the darkest parts of the image (open water and shadowed regions). 'J)he SNR of forest and clearings was estimated, respectively, at 12 dB and 18 dB at L-band, and 16 dB and 20 dB at C-band. With a 12-dB SNR, ρ_{SNR} is 0.94. The temporal coherence reduction is therefore less than 6%.

Geometric decorrelation occurs when the radar antennas do not point in the same direction during successive passes. When the plane of incidence of the radar illumination is the same for both antennas, the multiplicative factor modeling the geometric effect is

$$\rho_B = 1 - \frac{2\, B_\perp\, R_r \sin^2(\theta)}{\lambda\, R} \tag{2}$$

θ is the radar illumination angle with the horizontal, R_r is the spatial resolution in range, and R is the range distance. With $\theta = 42.8$", $R = 287$ km, and $B_\perp = 63$ m, we find ρ_B = 0.99 at L-band and 0.98 at C-band, i.e. < 2% reduction in coherence.

If the planes of incidence of the radar illumination from the two antennas arc squinted with respect to each other, forming a non-zero angle $\Delta\psi$ in the horizontal plane, coherence is

further reduced, The amount of decorrelation depends on the proportion of overlapping spectrum between the two images. Each SAR image has a bandwidth-limited azimuth spectrum centered at a doppler frequency $(2V_s \sin(\psi)/\lambda)$, where V_s is the velocity of the SAR platform. Neglecting the effect of $B_\perp$, the multiplicative factor modeling antenna squint is

$$\rho_\psi = \sqrt{1 - \frac{2 V_s \Delta\psi}{\lambda BW}} \tag{3}$$

The doppler bandwidth, BW, was 950 Hz at both L- and C-band. The doppler frequency of DT119.4,]35.4 and 151.4 were estimated at L-band during SAR processing at, respectively, -81, -144, and -4 Hz, yielding $\rho_\psi = 0.96$ at L-band and 0.81 at C-band.

These system effects cause an overall reduction in temporal coherence between 8 and 21% which cannot explain the spatial pattern exhibited in Figure 2 and the complete lack of coherence over forested areas. We conclude the low C-band coherence is a surface effect.

A surface effect implies a change in the nature and spatial distribution of the scatterers responsible for the Inca.sured radar returns inbetween the successive data takes. At C-band, radar scattering models and experimental evidence showed radar scattering is dominated by contributions from the smaller branches, twigs and needles or leaves of the upper canopy (e.g. Beaudoin et al., 1994). Random agitations in the position of small branches, twigs and leaves, for instance induced by wind, are therefore most likely to affect phase coherence. When the forest is frozen, the forest, canopy becomes more transparent because the dielectric constant is lower, and the role of the upper canopy conditions is diminished, Temporal coherence greater than 0.5 was observed in winter over boreal forests with ERS-1 SAR (Hagberg et al., 1995).

At 1,-band, the radar signals penetrate deeper into the forest canopy and interact with the larger-sized forest constituents such as tree-trunks and large branches, and the ground. The

larger objects and the ground are less subject to wind influence or random fluctuations in position, explaining why signal coherence is higher at L-band.

Topographic mapping at L-band

Height errors include uncertainties in range distance due to system clock timing, data sampling clock jitter or atmospheric propagation delays, system attitude and baseline separation, altitude of the spacecraft, and phase noise (Li and Goldstein, 1990). In examining local variations in surface height, however, height errors are dominated by phase noise and range delays through the atmosphere and the canopy.

The uncertainty in terrain height caused by phase noise is

$$\sigma_h = \frac{\lambda R \cos\theta}{4\pi B_\perp} \sigma_\phi \tag{4}$$

where phase noise, σ_ϕ, is

$$\sigma_\phi = \frac{1}{\sqrt{N}} \frac{\sqrt{1-\rho}}{\rho} \tag{5}$$

N is the number of samples used to average the interferometric phase, and p is the temporal coherence of the signal directly measured from the interferograms. With N = 36, for cleared areas (p = 0.85), we find $\sigma_\phi = 4^o$ and $\sigma_h = 5$ m. For the forest (ρ = 0.7), σ_h is 8 m.

As radar signals penetrate the forest canopy, they interact with a medium of dielectric constant greater than for air, increasing the electrical path length compared to that for clearings. At our site, above-ground biomass averages 30-40 kg/m^2 (Fearnside et al., 1992), wood density is 690 kg m^{-3} (Brown and Lugo, 1992) and tree height, h, averages 30 m (pers. observ., 1995), The volumetric fraction of forest is only 0.1 7%. Using van Beek (1967)'s refractive model, a dielectric constant of 20 for wood/leaves and 1 for air, we obtain an average dielectric constant of 1.01 for the forest. 'l'he one-way increase in electrical path length is 0.01 sin(θ) h or 26 cm, much less than phase noise.

Following Goldstein (1 995), we estimated the range delays due to atmospheric propagation by fitting a quadratic function through the phase data obtained from two interferograms. The residual phase disturbances are shown in Figure 4, scaled between -3 cm and +3 cm one-way range delay. The rms error in electrical path length is 1.2 cm, 5 times larger than observed in the California desert (Goldstein, 1995). larger values were expected in the more humid conditions of tropical rain-forests. With $B_\perp = 63$ **m,** these errors translate into 35 m uncertainties in surface height, occurring on a kilometer-scale basis, by far the largest source of height uncertainty, '1'o reduce these height errors to 1 m rms, $B_\perp$ must be > 2 km (Eq. (4)), which is still possible to usc at 1,-band.

Over small regions, a few pixels wide, atmospheric delays are uniform and height noise is dominated by phase noise. We compared the forest elevation with the elevation of adjacent clearings by selecting pairs of 3 x 3 boxes (100 m x 100 m) in forest and non-forest areas, along forest/non-forest transitions, separating the forest box from the non-forest box by 2-3 pixels to avoid possible edge effects. The mean and standard deviation in surface elevation of each box is plotted for each forest/non-forest pair in Figure 5. We make two observations: 1) the standard deviation in height of the forest is about twice larger than that for cleared areas; and 2) there is little contrast in height between forest and clearings.

The first observation is consistent with the high phase coherence of cleared areas, where surface scattering dominates. Phase coherence is lower in the forest, possibly because scattering interactions occur at various heights within the forest canopy, dispersing the position of the phase centers.

The second observation suggests the L-band phase centers are located only a few meters above ground. The average absolute difference between forest height and clear-cut height is 5 m, with a 5-m standard deviation. Edge effects arc negligible and radar penetration must

be considerable. Our field trip to Rondonia in October 1995 confirmed tree height averages 3(I m (e.g. Grace et al., 1995), and the transition to clearings is generally sharp (30 m in distance), as e.g. in the farmland near the scene center.

A recent airborne radar interferometry / laser altimetry experiment conducted in old-growth forests of the Pacific Northwest demonstrated the phase centers are already halfway between the canopy top and the ground at C-band (Rodriguez, et al., 1995). As signal attenuation decreases with decreasing radar frequency, the phase centers should be closer to the ground at 1,-band. In the SIR-C data, the phase centers are below half way down the forest profile (15 m), somewhere in the lower 8 m of tile forest. Whether the phase centers arc actually on the ground and L-band signals measure ground topography cannot be answered with these data, however. More accurate data collected from a dual-antenna instrument are required to answer that question,

Conclusions

imaging radars operating at long radar wavelengths offer strong and reliable temporal coherence for repeat-pass interferometric applications over vegetated terrain and could Inca.sure surface topography deep beneath thick vegetation canopies. Large scale applications of radar interferometry over the humid tropics must however be conducted in repeat-pass mode with kilometric baselines, or with two antennas operating simultaneously to avoid the limitations imposed by atmospheric delays.

References

Beaudoin A., rl. Le Toan, S. Goze, E. Nezry, A. Lopes, E. Mougin, C. C. Hsu, H. C. Han, J. A. Kong, and R. T. Shin, Retrieval of forest biomass from SAR data, *Int. , J. of Rem. Sens.*, 15 (14), 2777-2796, 1994.

Brown S. and A. Lugo, Above-ground biomass estimates for tropical moist forests of the Brazilian amazon, *Interciencia*, 17(4), 201-203, 1992.

Fearnside, P. M., N. Leal and F.M. Fernandes, Rainforest burning and the global carbon budget: biomass, combustion efficiency, and charcoal formation in the Brazilian amazon, *J. Geophys. Res.*, 98, 16,733-16,743, 1993.

Grace, J. and 11 others, Carbon dioxide uptake by an undisturbed tropical rain forest in southwest Amazonia, 1992 to 1993, Science, 270, 778-780.

Goldstein, R. M., Atmospheric limitations to repeat-track radar interferornetry, *Geophys. Res. Lett.*, 22(18), 2517-2520, 1995.

Hagberg, J .0., 1,. M. 11. Ulander, and J. Askne, Repeat-pass SAR interferometry over forested terrain, *IEEE Trans. on Geese. and Rem. Sens.* **33** (2), 331-340, 1995.

Li, F.K. and R.M. Goldstein, Studies of rnulti-baseline spaceborne interferometric synthetic aperture radars, *IEEE Trans. Geosc. Rem. Sens.*, 28(1), 88-97, 1990.

Rodriguez, E., manuscript in preparation, 1995.

Tucker, C. J., B. N. Holben, and T.E. Goff, intensive forest clearing in Rondonia, Brazil, as detected by satellite remote sensing, *Rem. Sens. Environ.*, 15:255-261, 1984.

Zebker, H .A. and J. Villasenor, Decorrelation in interferometric radar echoes, *IEEE Trans. on Geosc. and Rem. Sens.*, 30, 950-959, 1992.

Zebker, H .A,, T.G. Farr, R.P. Salaar and T.H. Dixon, Mapping the world's topography using radar interferometry, *IEEE Proc.*, 82, 1774, 1994.

van Beek, L. K. H., Dielectric behavior of heterogeneous systems, Ch. 7 in Progress *in Dielectrics*, (J. Birks, cd.), Heywood Books, London. 1967.

Figure 1. 1,-band (24-cm wavelength) radar image of a test site in Rondonia, Brazil. Image size is 46.1 km x 34.3 km, resolution is 30 m. North is pointing 148° right from the top of the image.

Figure 2. Phase coherence image for the image pair combining data takes 119.4 and **135.4** (one-day time interval) at (a) C-band (5.6-cm wavelength); and (b) L-band (24 cm). High correlation is bright, low correlation is dark.

Figure **3.** Elevation map derived from the L-band data. Hue and saturation are proportional to the inverse of the height, and intensity is proportional to the radar brightness at L-band. Terrain elevation ranges from 200 to 600 m.

Figure 4. One-way range delays caused by atmospheric perturbations, attributed to turbulent water vapor, color coded between -3 cm and +3 cm (dark blue to purple, orange, yellow, green and blue), and superimposed on the radar brightness of the terrain. Image size is 46.] km x 34.3 km.

Figure 5. Interferometric height of the forest versus non-forest using boxes 3 x 3 image pixels in size. Horizontal and vertical bars represent the standard deviation of the measurements.

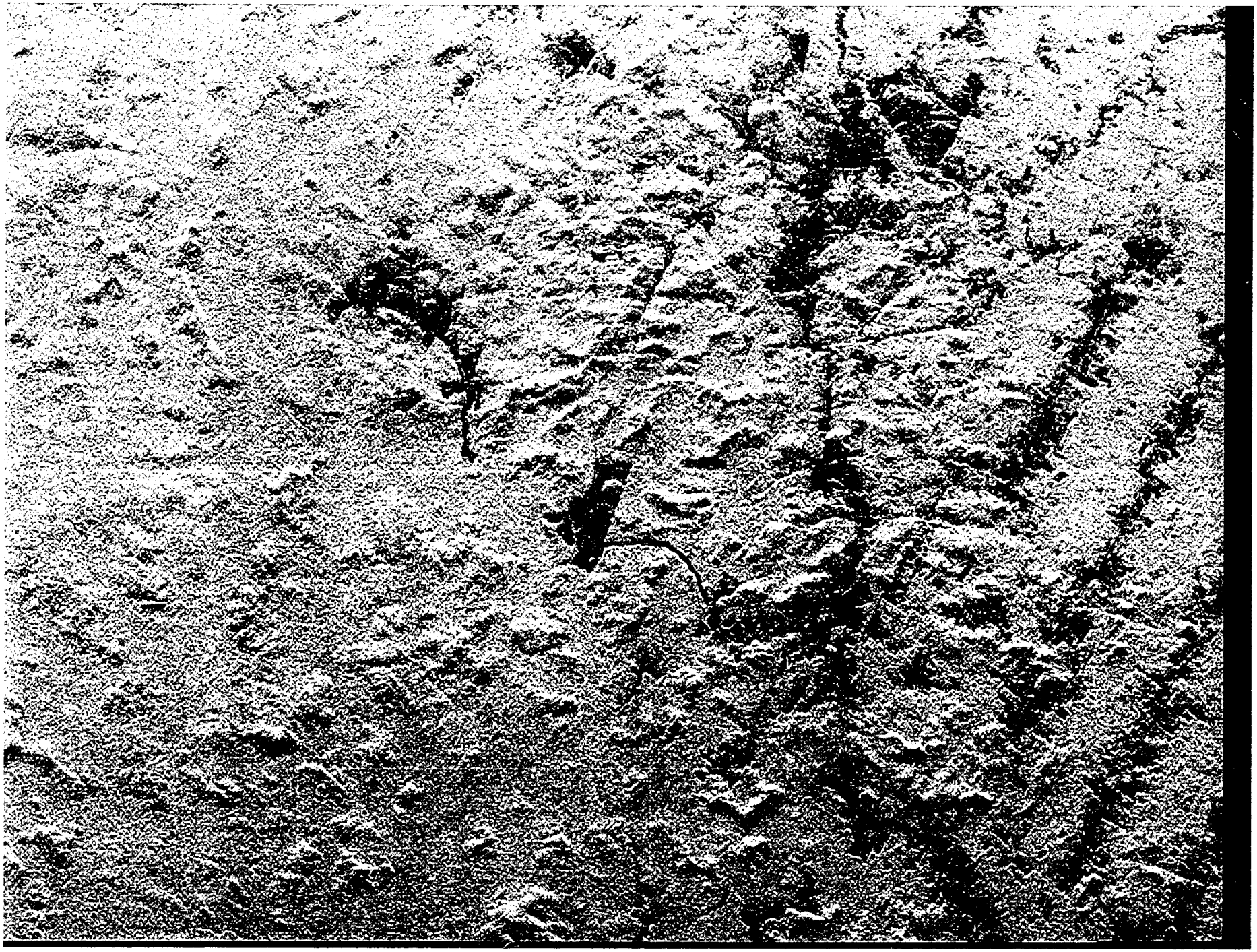

Figure 1

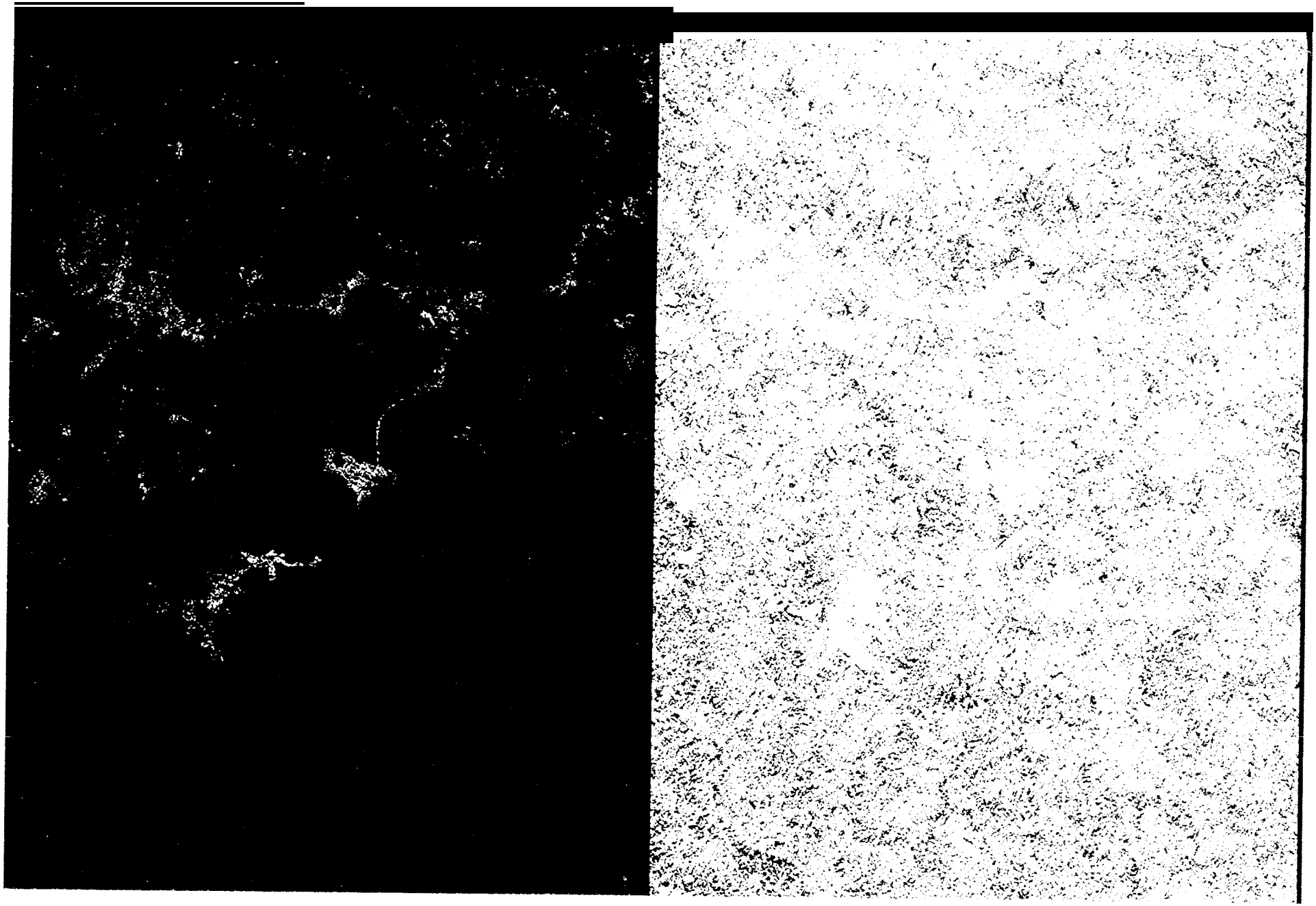

Figure 2a.

Figure 2b.

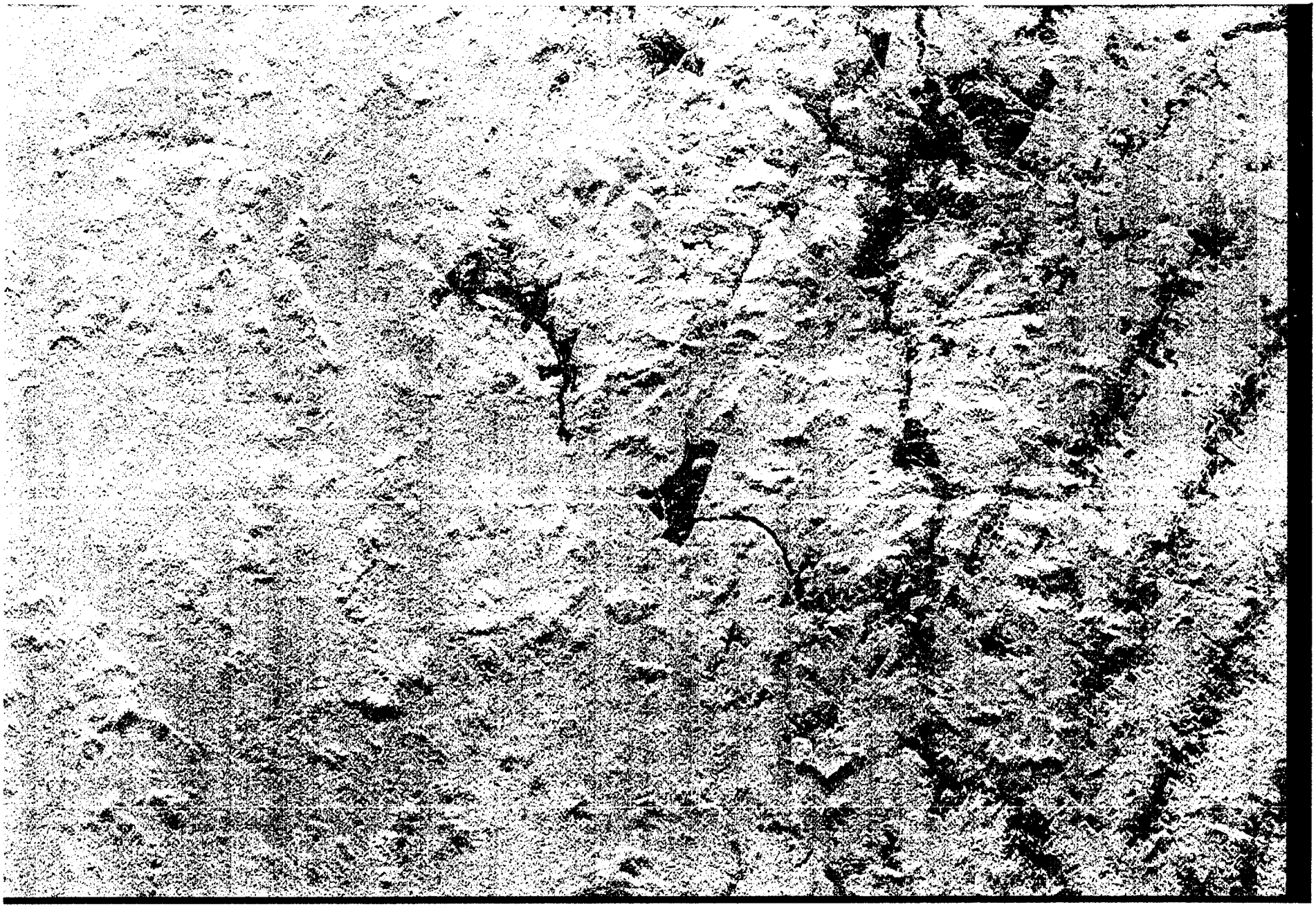

Figure 3.

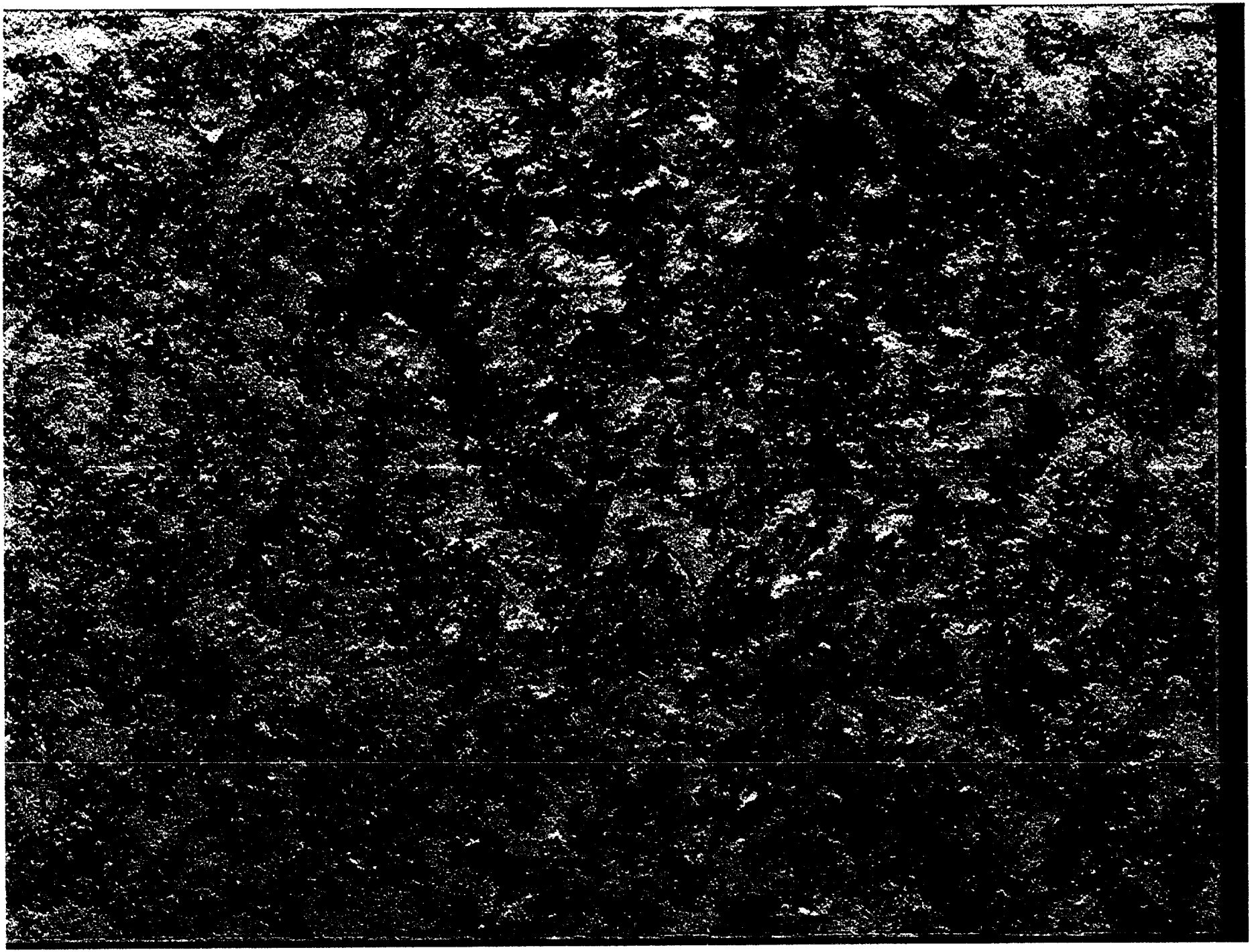

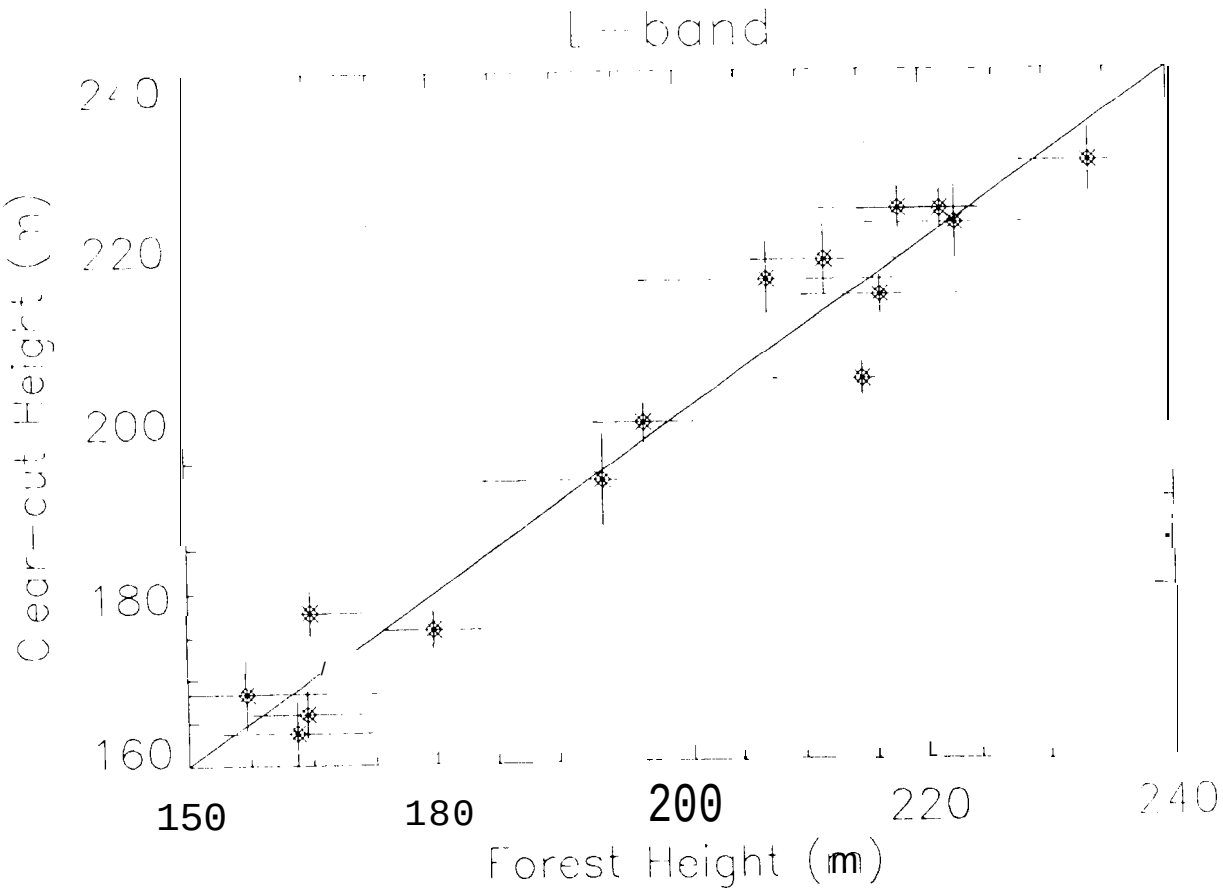

Figure 5.